

Photoemission Studies of Wurtzite Zinc Oxide*

R. A. Powell, W. E. Spicer, and J. C. McMenamin

Stanford Electronics Laboratories, Stanford University, Stanford, California 94305

(Received 29 March 1972)

Photoemission measurements have been made at photon energies between 7.8 and 11.6 eV on single crystals of wurtzite ZnO cleaved at pressures $<10^{-10}$ Torr. Additional measurements have been made from 11.6 to 21.2 eV in pressures of about 10^{-4} Torr. Important features of the density of states are deduced from the energy distributions of the photoemitted electrons. With respect to the top of the valence band, maxima in the conduction-band density of states are located at 8.5 ± 0.2 eV and 10.4 ± 0.2 eV, while two maxima in the valence-band density of states are found at -1.6 ± 0.2 eV and -2.8 ± 0.2 eV. The $3d$ band of Zn is located at -7.5 ± 0.2 eV. In addition, the valence band appears to be about 5 eV wide in contrast to widths of about 2–3 eV for other II-VI compounds such as ZnS, CdS, and CdSe. These features are in qualitative agreement with both a recent pseudopotential calculation by Bloom and, excepting the valence-band width and the location of the $3d$ levels, with the Green's-function (Korringa-Kohn-Rostoker) calculation of Rössler. The d bands are placed some 3 eV lower than predicted by Rössler's calculation; however, our assignment is in good agreement with recent x-ray photoemission measurements and is shown to be consistent with the low value of the effective number of free electrons n_{eff} calculated from the reflectivity. The effect of inelastic scattering due to pair production is also discussed.

I. INTRODUCTION

Over the last decade extensive ultraviolet (uv) photoemission studies have been made on many IIB-VIA compound semiconductors, including the selenides, sulphides, and tellurides of Zn and Cd.¹⁻³ Such measurements have yielded essential information on the higher-energy band structure of these materials; however, no corresponding studies of wurtzite (hexagonal) ZnO have been reported.

The purpose of the present study has been to use photoemission techniques to investigate the electronic structure of wurtzite ZnO over as wide a range of photon energies as possible. Of particular interest in the photoemission experiment were the location of the Zn $3d$ core states, the width of the upper valence bands, and structure in the conduction-band (CB) and valence-band (VB) density of states.

II. EXPERIMENTAL METHODS

The experiments reported here have been performed at room temperature on cleaved single-crystal ZnO. The most satisfactory cleavage plane was the (10 $\bar{1}$ 0) prism face parallel to the c axis. High-vacuum experiments (at pressures less than 10^{-10} Torr) were performed *in situ* using the cleaving chamber and vacuum system described by Derbenwick.⁴ The LiF window that seals the ultrahigh vacuum chamber will not, unfortunately, pass uv radiation having energy above 12 eV. Therefore, to extend these measurements beyond the 12-eV cutoff, a knock-off LiF window of the type developed by Krolikowski⁵ was used. In this case, the sample is first cleaved and studied in

the high vacuum chamber. Next, the LiF window is knocked off, exposing the sample to the low vacuum ($\approx 10^{-4}$ Torr) of the monochromator (McPherson model No. 225). There is then no window between the light source and the sample. A Hinteregger-type discharge lamp with a source gas of hydrogen was used as a continuum light source from the photoemission threshold near 8 eV to about 14.5 eV, while the sharp resonance lines of Ne I and He I were used at photon energies $\hbar\omega = 16.8$ and 21.2 eV, respectively. The energy distributions of photoemitted electrons (EDC's) were measured using the ac-modulated retarding-potential method of Spicer and Berglund⁶ as improved by Eden.⁷

III. PHOTOEMISSION STUDY OF ZnO

A. Energy Distributions of Photoemitted Electrons

In Figs. 1–5 we present selected EDC's for the photoemitted electrons. All the EDC's for $\hbar\omega < 12$ eV have been normalized to the absolute quantum yield shown in Fig. 6. That is, the area under an EDC equals the measured yield at that photon energy. However, it was not possible to take yield data for $\hbar\omega > 12$ eV owing to the absence of a calibrated phototube in this energy region. Higher-energy EDC's are therefore not normalized. Electron energies are stated relative to the valence-band maximum (VBM) and the energy scale has an instrumental uncertainty of ± 0.2 eV. Photoemission measurements were also made on ZnO using linearly polarized light in the range 8–10 eV, the electric vector being parallel and perpendicular to the c axis. No significant differences were ob-

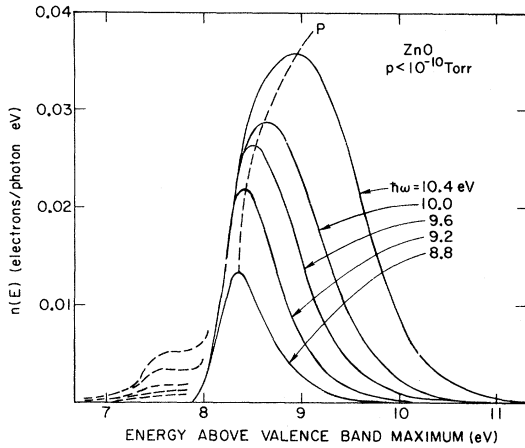


FIG. 1. Normalized energy distributions of the photoemitted electrons. $8.8 \leq \hbar\omega \leq 10.4$ eV. The dashed curves represent contributions to the EDC's from the uncleaned-sample sides.

served between these EDC's and EDC's taken using unpolarized light.

The value of the threshold voltage obtained from the zero intercept of the EDC's is found to be 7.8 ± 0.2 eV. Since the band gap of ZnO at room temperature is 3.34 eV, the electron affinity for an atomically clean (1010) surface of ZnO at room temperature is 4.5 ± 0.2 eV. It was also possible

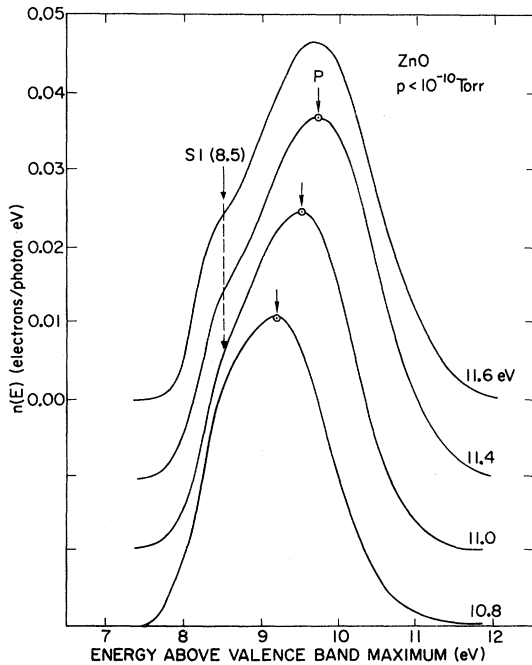


FIG. 2. Normalized energy distributions of the photoemitted electrons. $10.8 \leq \hbar\omega \leq 11.6$ eV.

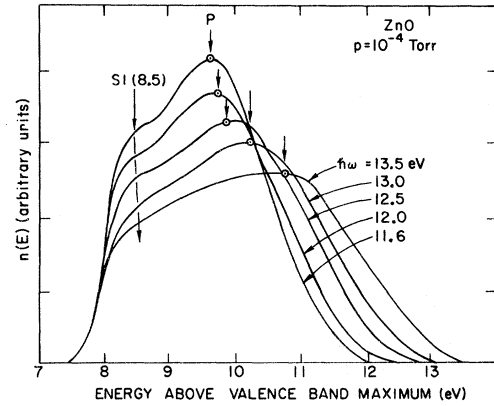


FIG. 3. Energy distributions of the photoemitted electrons. $11.6 \leq \hbar\omega \leq 13.5$ eV.

to accurately determine the collector work function by withdrawing the ZnO sample from the collector can and taking EDC's instead from the copper-coated back shutter. The work function of the collector was found in this way to be 5.0 ± 0.2 eV. Using this information, the Fermi level for our sample was placed about 3.2 eV above the VBM, which is reasonable for an *n*-type semiconductor, such as ZnO.

As the photon energy is increased above threshold, the first prominent feature to appear in the EDC's is the peak labeled *P* (Fig. 1). The position of *P* remains nearly constant at about 8.5 eV for photon energies in the range $\hbar\omega = 8.8$ –9.6 eV; however, the peak begins to move rapidly to higher final-state energies with increasing photon energy above 9.6 eV and becomes much more pronounced. By $\hbar\omega = 10.8$ eV (Fig. 2), the peak *P* has stopped growing and corresponds to transitions from initial states 1.6 eV below the VBM. This behavior probably reflects an increase in the VB density of states as photon energy probes deeper into the valence band. In fact, for photon energies in the range $\hbar\omega = 10.8$ –11.4 eV (Fig. 2), the location of *P* is approximately given by

$$E_p = \hbar\omega - 1.6 \text{ eV} . \quad (1)$$

The motion of *P* in accordance with Eq. (1) indicates that the peak is now due to transitions from a maximum in the VB density of states 1.6 eV below the VBM. As photon energy is increased above 11.4 eV, the initial states responsible for *P* lie deeper in the valence band. However, for $14.5 \geq \hbar\omega \geq 12.5$ eV (Figs. 3 and 4) the location of *P* is approximately given by

$$E_p = \hbar\omega - 2.8 \text{ eV} . \quad (2)$$

We therefore associate the peak *P* with VB structure. The motion of *P* in accordance with Eq. (2)

indicates that for $14.5 \geq \hbar\omega \geq 12.5$ eV, it is due to transitions from a maximum in the VB density of states located 2.8 eV below the VBM.

It is seen in Fig. 4(a), where the EDC's are plotted with respect to initial-state energies, that the peak *P* finally drops out of the EDC's for $\hbar\omega \geq 14$ eV. The disappearance of this piece of structure reflects the rapidly decreasing number of final states accessible from the maximum near -2.8 eV at these high photon energies.

A second piece of structure observed in the photoemission data for ZnO is a low-energy shoulder *S1* which first appears in the EDC's for $\hbar\omega \geq 10.8$ eV (Fig. 2). When it first appears, this shoulder represents transitions from initial states centered about -2.3 eV to final states lying about 8.5 eV above the VBM. By $\hbar\omega = 11.6$ eV, the shoulder is quite pronounced; however, it still remains centered at final-state energies near 8.5 eV.

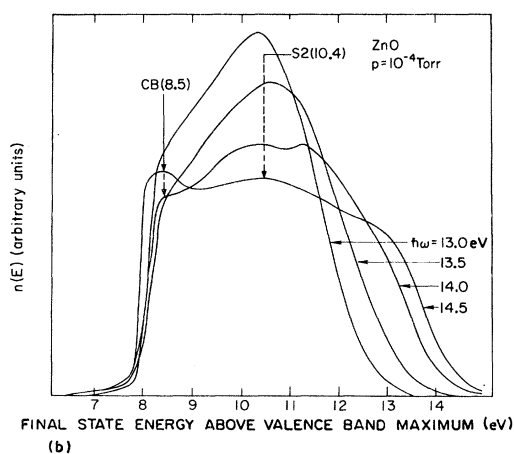
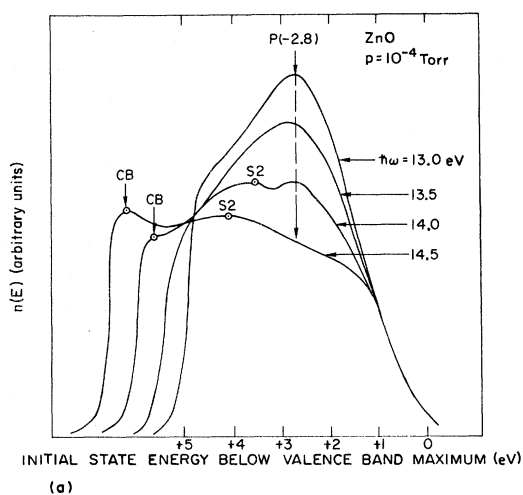


FIG. 4. Energy distributions of the photoemitted electrons plotted with respect to initial-state energy (a) and final-state energy (b). $13.0 \leq \hbar\omega \leq 14.5$ eV.

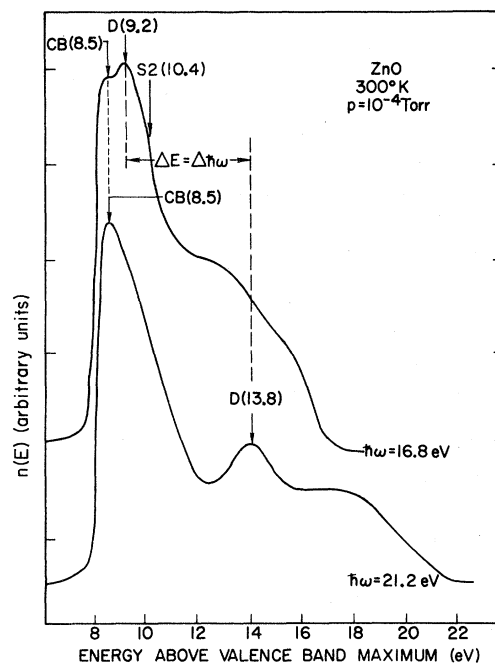


FIG. 5. Energy distributions of the photoemitted electrons for $\hbar\omega = 16.8$ eV and 21.2 eV. We suggest that peak *D* is due to transitions from the *d*-band density of states at -7.5 eV.

Therefore, we assign this shoulder to CB structure. It seems likely that *S1* is the result of transitions to a high-density-of-states region of the Brillouin zone near 8.5 eV as the photon energy probes deeper into the VB. If this is the lowest-lying high-density-of-states region in the ZnO conduction band, then it lies some 4–6 eV higher than corresponding structure found in the

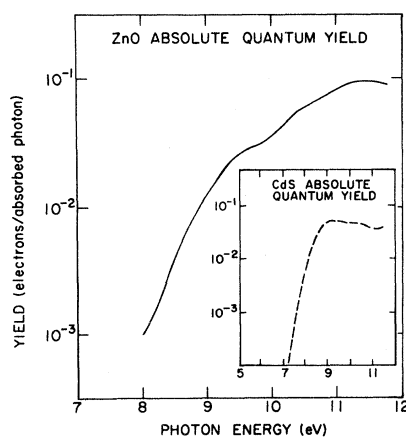


FIG. 6. Absolute quantum yield for a crystal of ZnO cleaved in high vacuum (pressure $< 10^{-10}$ Torr). For comparison, the quantum yield of a typical II-VI semiconductor CdS is shown (Ref. 2).

other II-VI compounds.

As photon energy is increased above 11.6 eV (Fig. 3), the shoulder S1 becomes less pronounced in the EDC's until by $\hbar\omega = 13.5$ eV it has completely disappeared. This behavior reflects a decreasing initial-state density as photon energy probes deeper into the VB. The disappearance of this shoulder for $\hbar\omega = 13.5$ eV suggests that the photon energy has now reached the very bottom of the VB density of states. In the EDC for $\hbar\omega = 13.5$ eV, photoemitted electrons that appear at 8.5 eV correspond to initial states 5 eV below the VBM.⁸ Since these initial states lie near the bottom of the VB, we estimate the minimum width of the VB in ZnO as 5.0 eV. This is 2–3 eV wider than the VB's in the other II-VI compounds.

At higher photon energies, $\hbar\omega \gtrsim 14$ eV, a peak CB is observed in the EDC's (Fig. 4). This new feature again corresponds to transitions into the high-final-state density at 8.5 eV. Direct excitation into these final states must be ruled out at the photon energies for which CB is first observed. Such transitions would involve coupling to states lying well below -5.0 eV, that is, deeper than the estimated width of the VB. Instead, we believe that this stationary peak of low-energy electrons CB is due to photoemitted electrons that have been inelastically scattered down from higher energies. It has also been possible in this way to explain similar structure observed in the EDC's of CdS and CdSe.² We expect such pair production (electron-electron scattering) to increase with the initial energy of the photoexcited electrons. In fact, for $\hbar\omega = 16.8$ eV and 21.2 eV (Fig. 5), the peak CB is seen to be much more pronounced than at 14.5 eV. Since the band gap of ZnO is 3.34 eV, we expect scattered electrons to appear 8.5 eV above the VBM for photon energies greater than about 11.8 eV. However, one must go to photon energies some 2 eV higher before the scattering peak CB is observed. This can be understood by noting that the number of electrons scattered down from some final-state energy is proportional to the number of photoexcited electrons initially available at that energy. For example, in the EDC's in Figs. 3 and 4(b), we see that for $\hbar\omega < 14$ eV those electrons escaping with final energies above 11.8 eV—the threshold for pair production into final states 8.5 eV above the VBM—comprise only a few percent of the total number of photoexcited electrons. However, by $\hbar\omega = 14$ eV this fraction has increased markedly to nearly 30% of the total. We therefore expect the number of electrons scattered down in energy to the density-of-states maximum at 8.5 eV to show a corresponding rise. This is in fact observed in the increased relative amplitude of CB for $\hbar\omega = 14.0$ eV.

A rather broad peak S2 which corresponds to

transitions into final states centered about 10.4 eV appears in the EDC for $\hbar\omega = 14$ eV [Fig. 4(b)]. For $\hbar\omega = 14.5$ eV, S2 is once again associated with final-state energies near 10.4 eV. We tentatively associate this structure with a peak in the CB density of states at 10.4 eV. For lower photon energies ($12 < \hbar\omega < 14$ eV) the contribution S2 cannot be separated out of the EDC's because of strong transitions from the VB—density-of-states maximum (-2.8 eV). The higher-energy EDC's tend to support this assignment for S2.

We present these unnormalized EDC's taken at the higher photon energies $\hbar\omega = 16.8$ and 21.2 eV in Fig. 5. In this high-energy region the reflectivity (which we later present as Fig. 7) is monotonically decreasing and notably lacking in structure. However, the EDC's are far from featureless. This behavior is not peculiar to ZnO. In many other materials, EDC's that are quite rich in structure have been observed at photon energies where the optical constants show little or no modulation.⁹

In this case, two well-resolved features CB and D, appear in both EDC's. We have discussed these high-energy EDC's in detail elsewhere¹⁰; however, for the sake of completeness, we reproduce these results in large part here.

At these high energies, most of the photoemitted electrons contribute to the pronounced scattering peak CB. We have assigned this peak earlier to inelastic scattering into a CB—density-of-states maximum at 8.5 eV. For lower photon energies, direct photoexcitation into this high-final-state density was observed (Figs. 2 and 3); however, by $\hbar\omega = 13.5$ eV, these interband transitions are nearly exhausted, the photon energy having probed to the bottom of the VB density of states. No struc-

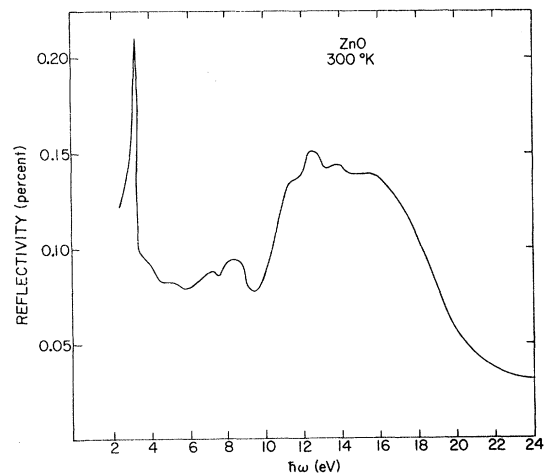


FIG. 7. Unpolarized reflectivity of ZnO measured by Hengehold *et al.* (Ref. 11).

ture is then observed in the EDC's at final-state energies near 8.5 eV until $\hbar\omega = 14$ eV when the stationary inelastic scattering peak CB first appears.

The rather weak shoulder S2 appearing at 10.4 eV in the EDC for $\hbar\omega = 16.8$ eV may similarly represent inelastic scattering down into a higher-energy density-of-states maximum at 10.4 eV. Although this feature is not resolved in the EDC for $\hbar\omega = 21.2$ eV, it may be argued that the asymmetric shape of the inelastic scattering peak is indirect evidence for the presence of such a shoulder.

We believe that the peak labeled *D*, which appears in the EDC for $\hbar\omega = 16.8$ eV at 9.2 eV is due to transitions from a high-VB density of states centered about 7.6 eV below the VBM. Because of the limitations of our uv source, it was not possible to follow the motion of *D* between 16.8 and 21.2 eV to confirm its origin in the VB. However, no corresponding peak at 9.2 eV is seen for $\hbar\omega = 21.2$ eV. This would have been the case if CB structure were responsible for *D*. Instead, a pronounced peak at 13.8 eV is seen in the EDC for $\hbar\omega = 21.2$ eV. Again, this structure corresponds to initial states near -7.6 eV (-7.4 ± 0.2 eV). On the basis of the EDC's we suggest that the peak *D* represents transitions from the Zn 3*d* bands, and further that these *d* bands are centered 7.5 ± 0.2 eV below the VBM.

B. Quantum Yield

In Fig. 6 we present the spectral distributions of the absolute quantum yield for $\hbar\omega < 12$ eV from a crystal of wurtzite ZnO cleaved in ultrahigh vacuum of less than 10^{-10} Torr. The yield below 10^{-3} electrons/photon has not been included because strong contributions from the uncleaved sample sides were observed in this region. Light intensities were measured using the absolute response of a calibrated Cs₃Sb phototube. By using the reflectivity shown in Fig. 7, the yields have been expressed as the total number of photoemitted electrons per incident *absorbed* photon. As can be seen from Fig. 6, the quantum yield of ZnO rises rather slowly with photon energy from the photoemission threshold near 8 eV and finally levels off some 4 eV higher. Such behavior contrasts that observed for other II-VI wurtzite compounds, e.g., CdSe and CdS (see insert in Fig. 6) in which the quantum yield rises almost twice as steeply from the threshold voltage and levels off within 2 eV of threshold.² It has been suggested that for ZnO either the VB's are wider¹¹ or that the corresponding CB structure lies higher¹² than in the other II-VI compounds. The present photoemission data show that for ZnO both these suggestions are valid. Consequently, one expects the rise of the ZnO yield near threshold to be

less sharp than other II-VI compounds.

It can also be seen from Fig. 6 that the quantum yield of ZnO in the range 8–12 eV is characterized by a narrow plateau or "notch" extending from about 9.5 to 10.5 eV. No such plateau has been observed in the measured yield of the other II-VI compounds.

The EDC's in this energy range (Fig. 1) show that for $\hbar\omega = 9.6$ eV most of the photoelectrons appear at final-state energies centered about the region of high-CB density of states at 8.5 eV. The corresponding initial states then lie relatively near the top of the VB centered about 1.1 eV below the VBM. Above $\hbar\omega = 9.6$ eV, the majority of the photoelectrons are being excited from initial states which move deeper in the VB with increasing photon energy to final states that are moving into the relatively low-density-of-states region between the two CB maxima at 8.5 and 10.4 eV. As photon energy probes deeper into the VB, the rapidly increasing initial-state density competes with the decreasing final-state density to produce the rather flat region seen in the yield. The corresponding feature in the optical data at these photon energies is a pronounced dip in the reflectivity at 9.6 eV (Fig. 7). It has been suggested that this dip might represent the upper limit for transitions between upper VB's and lowest CB's.¹³ This suggestion is consistent with the present photoemission data. In this connection, we might expect that the abrupt rise in the reflectivity for $\hbar\omega \geq 10.5$ eV indicates strong coupling to initial states near the peak in the VB density of states, 1.6 eV below the VBM. It is, in fact, seen from the EDC for $\hbar\omega = 10.4$ eV (Fig. 1) that most photoelectrons now have initial-state energies near -1.6 eV. The dominance of these transitions in the EDC's coincide with the abrupt rise in the quantum yield near 10.5 eV (that is, the end of the "notch").

The photoemission data have shown the VB in ZnO to be about 5 eV wide. Since the threshold voltage for photoemission is about 8 eV (Fig. 6), most photoelectrons should have energies above the vacuum level for photon energies $\hbar\omega \approx 12$ eV. However, the yield is seen to be only about 10% for $\hbar\omega$ near 12 eV. Some electrons are no doubt reflected at the semiconductor-vacuum interface; however, such a low value for the yield probably indicates that a large percentage of photoexcited electrons were inelastically electron-electron scattered during transport to the surface. Consequently, they do not have sufficient energy left to escape the crystal and do not appear in the measured yield. We recall that the higher-energy EDC's for ZnO were also modified owing to pair production and display a pronounced inelastic scattering peak CB (Fig. 5). In Sec. VI we estimate an average value for the electron escape depth in ZnO.

IV. CORE STATES IN ZnO

A. Location of the Zn 3d Bands

Based on structure observed in the higher-energy EDC's we have placed the Zn 3d bands 7.5 eV below the VBM. This assignment is in strong disagreement with the first published band calculation for ZnO by Rössler¹⁴ in which the band structure of ZnO exhibits *d* bands lying only about 4 eV below the VBM. For comparison, the *d* bands of the sulphides, selenides, and tellurides of Zn and Cd lie some 6–10 eV below the upper valence bands.¹⁴

In the past, it has proven difficult to use band-theoretical calculations to locate absolutely in energy such tightly bound states as filled *d* and *f* states. For example, considerable problems in this respect were found with the *d* bands in Cu as calculated¹⁵ with augmented plane waves and with the 4*f* levels in the rare earths.¹⁶ In view of the difficulty of such calculations, it is important to obtain an early comparison of these results with experiment. Unfortunately, the several experiments that have been done on ZnO do not agree on the location of the Zn 3d states.^{11–13,17,18}

In one experiment, the reflectivity spectrum of ZnO was measured for photon energies up to 20 eV above the fundamental edge (Fig. 7).¹¹ The effective number of free electrons n_{eff} was then obtained from a Kramers-Kronig analysis of this reflectivity spectrum;

$$n_{\text{eff}}(\omega) = (m/2\pi^2 Ne^2) \int_0^\omega x \epsilon_2(x) dx, \quad (3)$$

where N is the atom density of the crystal. n_{eff} was found to rise very slowly with photon energy, reaching only about two electrons per atom by 22 eV. Since there are ten *d* electrons per atom, the tentative conclusion from this behavior was that the onset of *d* band transitions had not been reached by 22 eV.

Electron-energy-loss measurements were also made over the energy range of band gap to 50 eV.¹¹ If one associates the dominant peak in this spectrum at 18.8 eV with a plasmon excitation, then a free-electron density of three per atom is obtained. Such a low value was taken as further evidence that the 3*d* electrons of Zn lie very deep in energy in ZnO.

Linearly polarized reflectivity measurements have recently been made on ZnO for photon energies in the range 3–25 eV, the electric vector being perpendicular and parallel to the *c* axis.¹³ We reproduce these results in Fig. 8.

The interpretation of these data was found to be in good agreement with the first published band structure for ZnO. For example, a peak observed in the reflectivity spectrum seen for both polarizations of light near 7 eV was assigned to transitions

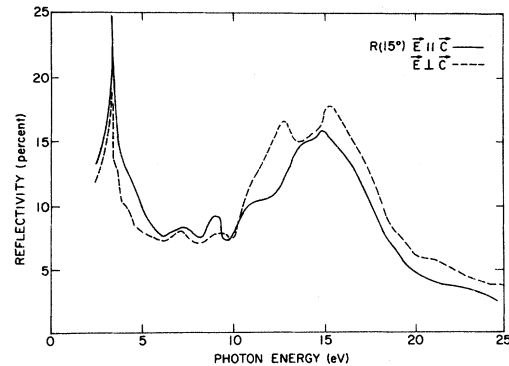


FIG. 8. Polarized reflectivity of ZnO measured by Klucker *et al.* (Ref. 13).

$d \rightarrow \Gamma_1$. Based on our photoemission data, the location of the Zn 3d states is such that transitions from *d* to Γ_1 could not occur for photon energies less than about 10 eV.

Another, more direct, determination of the energy levels of core electrons in ZnO has been made using the relatively new technique of x-ray-induced photoemission.¹⁷ The result of this study was that the Zn 3d level of ZnO lies 9.3 eV below the Fermi level (that is, 7.6 eV below the VBM, taking the Fermi level to lie at the center of the forbidden gap) and is no wider than in the other zinc chalcogenides. However, it has been pointed out¹² that this value included a systematic error in the electron-energy scale of about 1 eV.

A more recent determination using x-ray-induced photoemission places the Zn 3d core level at 10.34 eV below the Fermi level (that is, 8.6 eV below the VBM).¹² In addition, the spin-orbit splitting of this level was measured, the Zn 3d_{5/2} and 3d_{3/2} states being 10.04 and 10.79 eV, respectively, below the Fermi level. Unfortunately, we cannot confirm these spin-orbit results since the Zn 3d doublet could not be resolved in our photoemission data.

Finally, uv-induced photoemission measurements similar to ones we reported earlier¹⁰ have been carried out on ZnO for $\hbar\omega = 16.8$ and 21.2 eV.¹⁸ Although the location of the Zn 3d state determined by these new measurements (8.5 ± 0.4 eV below the VBM) disagrees slightly with our measured value of 7.5 ± 0.4 eV, both values are considerably lower than that predicted by Rössler's band calculation.

These values, obtained from uv-induced photoemission, can be reconciled with the negative result obtained from the behavior of n_{eff} by taking into account the atomic nature of the tightly bound *d* electrons. Many workers have noted that the matrix element between the conduction band and such tightly bound valence states increases very

slowly with photon energy.¹⁹ In fact, the oscillator sum rule is not exhausted until an energy many times greater than the threshold for such transitions is reached. In particular, Beaglehole²⁰ has applied this argument to the noble metals to explain the small contribution of the 3*d* electrons to n_{eff} . For the reader's benefit, a similar argument is briefly described for ZnO.

Using a simple model, we represent the Zn 3*d* VB wave functions by an appropriate tight-binding sum

$$\psi_{3d} = (NV)^{-1/2} \sum_i e^{i\vec{k}\cdot\vec{R}_i} \varphi_{3d}(\vec{r} - \vec{R}_i), \quad (4)$$

where φ_{3d} is an atomic 3*d* core state. The matrix element for a direct transition from an initial 3*d* state to an excited CB state, which we consider as a plane wave state $\psi_f = V^{-1/2} e^{i\vec{k}\cdot\vec{r}}$, is then given by

$$\langle \psi_{3d} | \nabla_{\vec{r}} \psi_f \rangle = N^{1/2} \int_{\text{unit cell}} \vec{k} e^{i\vec{k}\cdot\vec{r}} \varphi_{3d}^*(\vec{r}) d^3r. \quad (5)$$

From the partial wave expansion of the free-electron wave function

$$\begin{aligned} \psi_f &= V^{-1/2} e^{i\vec{k}\cdot\vec{r}} \\ &= V^{-1/2} \sum_{L=1}^{\infty} i^L (2L+1) j_L(kr) P_L(\cos\theta), \end{aligned} \quad (6)$$

it can be seen that the higher angular momentum components increase with increasing final-state energy. Now the dipole selection rules require that $\Delta L = \pm 1$. However, it has been pointed out¹⁹ that the oscillator strength for transitions with $\Delta L = \pm 1$ is roughly an order of magnitude greater than for $\Delta L = -1$. Thus, to get strong transitions from the Zn 3*d* bands (that is, to get appreciable *f*-like behavior in the final-state wave function), one must go to energies that may be considerably above the threshold for such transitions.

Our work indicates then that the onset of *d*-band transitions occurs in ZnO for $\hbar\omega$ substantially lower than 22 eV. However, at these low energies the contribution of *d*-band transitions to n_{eff} is too small to separate out. Consequently, one would not expect the *d* electrons to contribute strongly to a collective oscillation at $\hbar\omega = 18.8$ eV.

B. Contribution of *d* Bands to Reflectivity and $\epsilon_2\omega^2$

We now consider the effect of *d*-band transitions on the higher-energy reflectivity of ZnO.

The reflectivity spectrum of ZnO (Fig. 7) is unlike that of any other II-VI compound in that the major structure begins for photon energies $\hbar\omega \gtrsim 10$ eV.¹¹ In wurtzite CdS, CdSe, and ZnS, for example, the interband oscillator strength is nearly used up by this energy and the reflectivity is rapidly decreasing and essentially devoid of structure.²¹ In contrast, the reflectivity of ZnO is seen to rise

sharply for $\hbar\omega \approx 10$ eV and exhibits an extremely broad asymmetric peak. The rapid rise of the reflectivity above 10 eV has been discussed earlier in connection with the "notch" in the quantum yield and was attributed to an increasing number of transitions from the high-VB density-of-states region near -1.6 eV.

We suggest that the reflectivity of ZnO displays a characteristic broadened peak because when the onset of *d*-band transitions ($3d \rightarrow \Gamma_1$) occurs for $\hbar\omega \approx 11$ eV, transitions from the lower VB's are still contributing strongly to the reflectivity. Of all the II-VI compounds, this situation is peculiar to ZnO. In CdS, for example, the onset of transitions from the Cd 4*d* states occurs when transitions from the upper VB's are nearly exhausted.²² Consequently, there is an abrupt rise in the reflectivity corresponding to transitions $4d \rightarrow \Gamma_1$. It is then relatively easy to separate out the contribution of the *d*-core levels to the higher-energy reflectivity. Unfortunately, this is not the case for ZnO.

At this point it is useful to consider the transition strength $\epsilon_2\omega^2$ which is presented in Fig. 9. We have calculated $\epsilon_2\omega^2$ using values of the imaginary part of dielectric function ϵ_2 obtained by Hengehold *et al.*¹¹ The shoulder at $\hbar\omega \approx 11.2$ eV suggests the onset of *d*-band transitions ($3d \rightarrow \Gamma_1$). We have not, however, assigned structure observed in $\epsilon_2\omega^2$ in the region 12–15 eV to *d* transitions since the density of final states accessible from the 3*d* states at these photon energies is probably very low. At higher energies, a rather weak shoulder observed near 16 eV suggests that transitions are occurring from the *d* bands (-7.5 eV) to the high-CB density of states near 8.5 eV. The transition strength then suddenly levels off at 20 eV and begins to increase slightly. This behavior

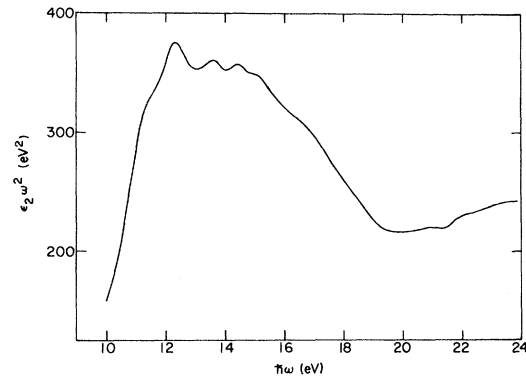


FIG. 9. Transition strength of ZnO—the imaginary part of the dielectric function times the square of the photon energy. We evaluated this function using optical data obtained by Hengehold *et al.* (Ref. 11).

seems unrelated to core-state transitions. Rössler, however, has theoretically located p -antibonding states some 17 eV above the VBM.¹⁴ The onset of transitions from p -bonding to these p -antibonding states would then occur for $\hbar\omega \approx 20$ eV. The peculiar behavior of $\epsilon_2\omega^2$ near 20 eV may then mark the beginning of transitions to these high-lying p -antibonding states.

V. BAND STRUCTURE OF ZnO

Recently, renewed interest in ZnO has been generated by the first published band structure for that material which we reproduce in Fig. 10. According to this calculation by Rössler,¹⁴ using the Korringa-Kohn-Rostoker (KKR) method,²³ the band structure of ZnO exhibits a broad free-electron-like lowest conduction band, relatively wide (1.6 eV) Zn 3d levels lying closely below the upper VB's, and p -antibonding CB states 17 eV above the VBM.

The Green's function (KKR) approach appears to have been reasonably successful in predicting the electronic band structure of such cubic II-VI semiconductors as ZnS, ZnSe, and ZnTe.²⁴ This method involves the use of an *ad hoc* potential with only a single adjustable parameter which is adjusted to obtain the correct band gap. Such a calculation, then, does not require the input of a great deal of experimental data. Indeed, it is significant that for ZnO the first calculated band structure actually precedes much of the relevant optical data. In this case, experimental results will be particularly valuable in confirming or correcting the theoretical model used in the band calculation.

Since the threshold for photoemission from our ZnO sample was nearly 8 eV, it was not possible to observe CB states lying less than this energy above the VBM. We were therefore unable to confirm the shape of the lowest conduction band as predicted by the KKR theory (Fig. 10).

Experimentally determined maxima in the VB and CB density of states are sketched in Figs. 10

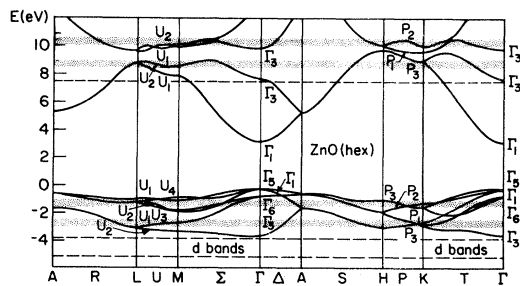


FIG. 10. KKR band structure for wurtzite ZnO (Ref. 14). The shaded sections represent maxima in the VB and CB density of states as determined from the photoemission experiment. The vacuum level is indicated by the dashed line at 7.8 eV.

and 11. As noted earlier, the Zn 3d states were found to lie 7.5 eV below the VBM, some 3 eV below that predicted by the KKR calculation. Except for the location of these core states, it appears from Fig. 10 that the KKR calculation is in good agreement with the experimental maxima. The regions of the Brillouin zone which one might associate with these high-state densities are probably the nearly flat region along U extending from the zone edge at L to the zone face at M and the region along P . There is considerable disagreement, however, between the calculated VB width (3.5 eV) and the value (5.0 eV) obtained from the photoemission experiment.

In Fig. 11 we present a recent pseudopotential band-structure calculation of ZnO by Bloom²⁵ (the notation of Rashba²⁶ has been used so that Γ_5 , Γ_6 correspond to Rössler's Γ_6 , Γ_5). In the pseudopotential theory, a local repulsive potential is constructed that cancels the crystal potential in the core region resulting in a smooth pseudopotential. Hence, such a calculation cannot describe d bands at all. However, such an approach may be justified for ZnO if the Zn 3d band lies deep enough to produce a negligible perturbation on the higher-energy bands. As with the KKR calculation, the pseudopotential calculation seems to be in general agreement with the experimentally determined maxima in the VB and CB density of states. From Fig. 11, it appears that the region of the Brillouin zone along P is associated with the high-CB-state density near 8.5 eV while the region along U is associated with the high-CB-state density near 10.4 eV. Realistically, a density-of-states calculation is needed to determine how good in fact this agreement is. In this connection, a calculation of EDC's based on the theoretical band calculations would be most useful. We further note that the calculated valence-band width of 5.0 eV is in agreement with the experimental value. It is not surprising that the VB in ZnO is considerably wider than that of any other II-VI compound. It is seen from Table I, where bond lengths are given for several II-VI compounds, that the O-O distance for ZnO is smaller by about 1 Å than the Se-Se, Te-Te, or S-S distances in the other compounds. The valence-band width in these IIB-VIA materials depends strongly on the wave-function overlap of the group-VIA atoms. Based on the short bond length in ZnO, we expect the VB wave-function overlap to be greater in that material than in the other II-VI compounds. Hence, we expect the VB width to be much wider for ZnO than for the other II-VI compounds.

VI. ESTIMATE OF ESCAPE DEPTH

By making the assumption that no electrons which pair produce (electron-electron scatter) can

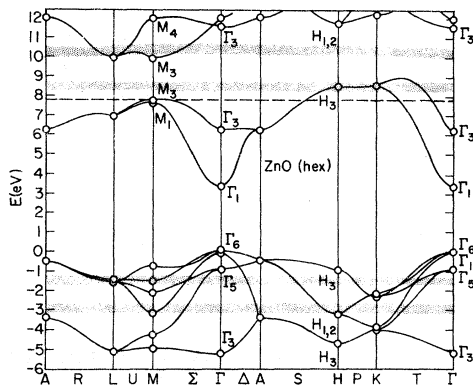


FIG. 11. Pseudopotential band calculation for wurtzite ZnO (Ref. 24). The shaded sections represent maxima in the VB and CB density of states as determined from the photoemission experiment. The vacuum level is indicated by the dashed line at 7.8 eV.

escape from the crystal, we can easily estimate an average escape depth for our high-vacuum-cleaved ZnO sample. Since the minimum energy loss through pair production is equal to the band gap of 3.34 eV, and threshold is about 7.8 eV; this assumption will be valid for photon energies less than about 11 eV. In this case, the yield Y can be shown to be approximately²⁷

$$Y \approx 0.5 \alpha L T / (1 + \alpha L), \quad (7)$$

where $\alpha L / (1 + \alpha L)$ is the probability that an electron photoexcited about the vacuum level will not pair produce during transport to the surface and T is the surface-transmission probability. That is, a fraction T of all the electrons reaching the surface escape into the vacuum. The factor of 0.5 accounts for those photoexcited electrons initially heading away from the semiconductor surface. We can see from the EDC for $\hbar\omega = 10.8$ eV (Fig. 2) that the photoemitted electrons have an average energy of about 9.2 eV corresponding to emission from the peak in the VB density of states at about -1.6 eV. At $\hbar\omega = 10.8$ eV, the absolute quantum yield is 0.047 for our ZnO sample (Fig. 6). If we make a reasonable assumption that T lies between 0.25 and 0.50 for electrons about 9.2 eV above the VBM—some 1 eV above threshold—then from Eq. (7), $0.23 < \alpha L < 0.61$. The absorption coefficient α can be calculated from the value of the extinction coefficient k at $\hbar\omega = 10.8$ eV by using $\alpha = 4\pi k / \lambda$. For ZnO, the extinction coefficient has been obtained by Hengehold *et al.*¹¹ from a Kramers-Kronig analysis of the measured reflectivity. We therefore calculate that $\alpha = 6.02 \times 10^5 \text{ cm}^{-1}$. Using this value for α , we find that the escape depth for an electron in ZnO 9.2 eV above the VBM is 30–100 Å. This value is roughly the same magnitude as es-

cape depths calculated in a similar way for high-vacuum-cleaved CdS, CdSe, and CdTe.²

VII. CONCLUSIONS

In conclusion then, photoemission measurements have been used to determine important features in the band structure for ZnO. In analyzing the photoemission data no distinction has been made between direct and nondirect transitions because the data represent transitions between relatively "flat" bands (Figs. 10 and 11).

Based on the disappearance of structure in the EDC's as photon energy probes below the VB density of states, we have set the bottom of the valence band. An estimate of 5.0 eV has been obtained for the VB width. This is several volts wider than in the other II-VI compounds.

Five maxima in the EDC's have been associated with maxima in the density of states.

Two maxima in the CB density of states are located at 8.5 ± 0.2 eV and 10.4 ± 0.2 eV above the VBM. Maxima also occur at -1.6 ± 0.2 eV, -2.8 ± 0.2 eV, and at -7.5 ± 0.2 eV, where the zero of energy is taken as the VBM. The former two maxima occur in the VB density of states, whereas the latter one is associated with the 3d levels of Zn. We have summarized the structure observed in the EDC's for ZnO in Fig. 12. In this plot, structure related to maxima in the CB density of states plots horizontally (i. e., does not move with photon energy) while structure related to maxima in the VB density of states moves with photon energy (i. e., $\Delta E = \Delta\hbar\omega$).

With two notable exceptions—the location of 3d core states and the VB width—the features of the electronic band structure found in this work are in general agreement with the two calculated band structures for ZnO.^{14,25} Both the KKR band calculation by Rössler and a recent pseudopotential calculation by Bloom exhibit VB and CB densities of states which seem in reasonable agreement with

TABLE I. Bond lengths of several selected IIB-VIA compounds.

Compound	Crystal structure	Bond length (Å) ^a
ZnO	Wurtzite	3.25
ZnS	Wurtzite	3.81
ZnS	Zinc blende	5.41
ZnSe	Wurtzite	3.98
ZnTe	Zinc blende	6.09
CdO	Rocksalt	4.69
CdS	Wurtzite	4.13
CdS	Zinc blende	5.82
CdSe	Wurtzite	4.30
CdTe	Zinc blende	6.48

^aBond lengths are taken from Ref. 28.

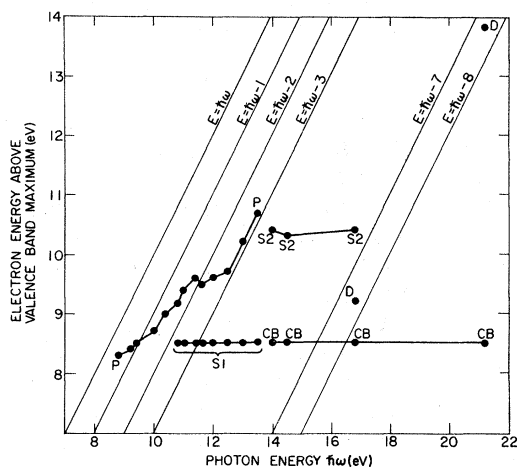


FIG. 12. Structure plot summarizing the structure in the ZnO-energy-distribution curves (Figs. 1-5). The slanted lines are lines of constant initial-state energy.

the photoemission results above. Both calculations predict fairly wide VB's; however, in this case agreement with the pseudopotential calculation (5.0 eV) is considerably better than with the KKR calculation (3.5 eV).

The location of the Zn 3d core states determined by the photoemission experiment is some 3 eV lower

than predicted by the KKR calculation. Our value is in reasonable agreement with recent uv- and x-ray-induced photoemission measurements,^{12,17,18} and is shown to be consistent with the low calculated value of n_{eff} at $\hbar\omega = 22$ eV obtained from the reflectivity.¹¹ It will, however, be necessary to reinterpret the reflectivity spectrum where *d*-band transitions have been previously assigned.¹³ In addition, the absolute energy of the *d* bands and the CB maxima will have to be taken into account by any subsequent band calculation.

It would be useful to compare the results of the photoemission experiment with a theoretical calculation of the density of states for ZnO or, more directly, with theoretically calculated EDC's. Such a calculation could be based on Rössler's KKR band structure but need not consider the *d* bands. Alternately, such a calculation could be based on a method which does not describe *d* states (e.g., a pseudopotential band structure such as Bloom's). By not taking the *d* bands into account, the calculation is made much less difficult.

ACKNOWLEDGMENTS

The authors are indebted to Phillip C. McKernan for fabricating the LiF knock-off window used in this work. We also wish to thank Dr. S. Bloom for allowing the inclusion of his pseudopotential calculation in this paper.

*Work supported by NASA and the Advanced Research Projects Agency through the Center for Materials Research at Stanford University, Stanford, Calif.

¹J. L. Shay and W. E. Spicer, Phys. Rev. **175**, 741 (1968).

²J. L. Shay and W. E. Spicer, Phys. Rev. **169**, 650 (1968).

³J. L. Shay, dissertation (Stanford University, 1966) (unpublished).

⁴G. F. Derbenwick, dissertation (Stanford University, 1970) (unpublished).

⁵W. F. Krolikowski, dissertation (Stanford University, 1970) (unpublished).

⁶W. E. Spicer and C. N. Berglund, Rev. Sci. Instr. **35**, 1665 (1964).

⁷R. C. Eden, Rev. Sci. Instr. **41**, 252 (1970).

⁸The relatively large number of photoelectrons that are observed near 8.5 eV when the shoulder S2 disappears ($\hbar\omega = 13.5$ eV) represent once scattered electrons. As photon energy increases above 11.6 eV, direct photoexcitation into the 8.5-eV CB maximum decreases while the number of electrons inelastically scattered down from higher energies to the 8.5-eV maximum increases.

⁹W. E. Spicer and R. C. Eden, in *Proceedings of the Ninth International Conference on the Physics of Semiconductors, Moscow, 1968*, edited by S. M. Rykin and Yu. V. Shmartsev (Nauka, Leningrad, 1968).

¹⁰R. A. Powell, W. E. Spicer, and J. C. McMenamin, Phys. Rev. Letters **27**, 97 (1971).

¹¹R. L. Hengehold, R. J. Almasy, and F. L. Pedrotti, Phys. Rev. B **1**, 4784 (1970).

¹²C. J. Vesley and D. W. Langer, Phys. Rev. B **4**, 451

(1971).

¹³R. Klucker, H. Nelkowski, Y. S. Park, M. Skibowski, and T. S. Wagner, Phys. Status Solidi **B45**, 265 (1971).

¹⁴U. Rössler, Phys. Rev. **184**, 733 (1969).

¹⁵E. C. Snow, Phys. Rev. **171**, 785 (1968).

¹⁶J. O. Dimmock, A. J. Freeman, and R. E. Watson, in *Optical Properties and Electronic Structure of Metals and Alloys*, edited by F. Abelès (North-Holland, Amsterdam, 1966), p. 237.

¹⁷D. W. Langer and C. J. Vesley, Phys. Rev. B **2**, 4885 (1970).

¹⁸C. J. Vesley, D. W. Langer, and R. L. Hengehold (unpublished).

¹⁹V. Fano and J. W. Cooper, Rev. Mod. Phys. **40**, 441 (1968).

²⁰D. Beaglehole, in Ref. 16, p. 154.

²¹M. Cardona and G. Harbeke, Phys. Rev. **137**, A1467 (1965).

²²N. B. Kindig and W. E. Spicer, Phys. Rev. **138**, A561 (1965).

²³J. Koringa, Physica **13**, 392 (1947); W. Kohn and N. Rostoker, Phys. Rev. **94**, 1111 (1954).

²⁴P. Eckelt, O. Madelung, and J. Trensche, Phys. Rev. Letters **13**, 656 (1967); P. Eckelt, Phys. Status Solidi **23**, 307 (1967).

²⁵S. Bloom (unpublished).

²⁶E. I. Rashba, Fiz. Tverd. Tela **1**, 407 (1959) [Sov. Phys. Solid State **1**, 368 (1959)].

²⁷W. E. Spicer, J. Phys. Chem. Solids **22**, 365 (1961).

²⁸R. W. G. Wyckoff, *Crystal Structures* (Wiley, New York, 1963).